Available online at www.sciencedirect.com
ScienceDirect
Physica A 379 (2007) 23–31
PHYSICA A
www.elsevier.com/locate/physa

Conformations of isolated ampholytic dendrimers in solutions

Edward G. Timoshenko[a,*], Yuri A. Kuznetsov[a], George E. Simonov[b]

[a]*Laboratory of Biomolecular Conformations, School of Chemistry and Chemical Biology, University College Dublin, Belfield, Dublin 4, Ireland*
[b]*CSIC, Moscow State University, Moscow 119992, Russia*

Received 7 November 2006
Available online 1 February 2007

Abstract

We study the conformations of isolated trifunctional ampholytic dendrimers in solutions. For the previously homo-dendrimer case studied in the literature, we discuss the issues of density profiles, the existence of a cavity, backfolding, bond stretching and scaling laws for the dendrimer size across the good-to-poor solvent transition. We then consider the effect of introducing monomer charges in the outermost generation opposite to those in the interior generations in an electrically neutral overall ampholytic co-dendrimer.

Keywords: Dendrimer; Polyampholyte; Conformation

1. Introduction

Regularly hyper-branched macromolecules (dendrimers) have received a great deal of attention in the past few years [1]. Due to the large number of peripheral monomers and the high degree of control over their structure, dendrimers have found applications as promising vectors for drug delivery [2] and for catalysis [3], to mention just a few. Many drug molecules are quite hydrophobic, but reaching the desired targets involves travelling through aqueous solutions.

Micellar systems in aqueous solution can dissolve the drug molecules within their hydrophobic interior, while the polar exterior of the micelle provides enough water solubility to dissolve the micelle. However, standard micellar systems rely on maintaining the so-called 'critical micelle concentration' (CMC) upon dilution in e.g., the bloodstream. Many of these systems can be quite kinetically stable, and hence can still be of value. However, amphiphilic co-dendrimers have been found to form so-called 'unimolecular micelles' which, by definition, do not have a CMC, and, therefore, may have some promise as drug delivery vehicles. Presently the use of amphiphilic co-dendrimers as drug delivery vectors is being evaluated by several groups [2].

*Corresponding author.
E-mail addresses: Edward.Timoshenko@ucd.ie (E.G. Timoshenko), gesimonov@yahoo.co.uk (G.E. Simonov).
URL: http://www.brightstar.ucd.ie.

0378-4371/$ - see front matter
doi:10.1016/j.physa.2006.12.055

The well-defined structures adopted by dendrimers also make them promising building blocks in supramolecular chemistry [4], where well-defined, 'shape-persistent architectures' [5] are highly desirable. While flexible homo-dendrimers adopt highly spherical structures [6], there is also interest in obtaining well-defined non-spherical shapes [7]. By using more than one type of monomer, i.e., co- (or hetero-) dendrimers [8], it should be possible to design different novel structures from dendrimers.

An important feature of the dendrimers is their sensitivity in response to changes of the pH, for dendrimers with ionisable groups [9], and of the temperature, which affects the solvent quality.

2. Nomenclature used

We adopt the same notations as in Refs. [6,7]. We shall consider a dendrimer as consisting of G generations, each of which is separated by D spacers, with an F_0 functional core (generation $g = -1$) and all the other branch points of functionality F. For simplicity, we treat each monomer as an identical sphere of diameter d, but we can distinguish between solubilities and charges of different chemical repeating units. If $D = a$ and $G = b$, we shall denote such a dendrimer as $DaGb$, as in Refs. [6,10]. The total number of monomers, N, will be $N = 1 + F_0 D((F-1)^{G+1} - 1)/(F-2)$. We will consider the case where all branch points have a functionality of 3, i.e., $F = F_0 = 3$. Sometimes it is instructive to distinguish between monomers in distinct 'dendrons' or primary branches. We can consider the dendrimers discussed here as comprising three identical dendrons attached to a single core monomer.

Due to the high symmetry of dendrimers, it is convenient to average monomer–monomer pairs over their symmetry equivalent classes. Hence, as previously [6], we will describe monomers in terms of their shell radial index, ρ, or 'span', i.e., the number of bonds separating a monomer from the core monomer.

For ampholytic dendrimers we shall consider the periphery monomers as positively charged with charge $|e|$ and the interior monomers as negatively charged with charge $-|e|\delta$, where $\delta = N_+/N_- \gtrsim 1$ is a number quite close to unity[1] to ensure the overall electrical neutrality of the dendrimer.

In the case of amphiphilic co-dendrimers we have a selective solvent for the periphery and interior generation monomers. Thus, we will distinguish two types of co-dendrimers, one where the hydrophobic (H) monomers are in the outermost generation and the rest of the monomers are polar (P), 'outer-H', and the opposite case, 'inner-H' as in Refs. [11,12].

3. The model and simulation techniques

Monte Carlo (MC) simulations were carried out using the standard Metropolis algorithm. All simulations were carried out in continuous space to avoid producing any lattice artefacts, which can be particularly problematic for highly branched systems as discussed in Refs. [6,11,12].

We use the following Hamiltonian of the system [11,12] and homo-dendrimers [6]:

$$\frac{H}{k_B T} = \frac{3}{2\ell^2} \sum_{i \sim j} \kappa_{ij} (\mathbf{X}_i - \mathbf{X}_j)^2 + \frac{1}{2} \sum_{ij,\ i \neq j} U_{ij}^{(nonb)}(|\mathbf{X}_i - \mathbf{X}_j|), \tag{1}$$

where $\mathbf{X}_i$ are the monomer coordinates and ℓ is the statistical bond length.[2] The first term represents the connectivity of the polymer with harmonic springs of strength κ_{ij} introduced between any pair of connected monomers (which we denoted by $i \sim j$). It should be noted that we define a 'monomer' in relation to the Kuhn length of the polymer. This beads-on-spring model therefore disregards more detailed bonded interactions, such as angular and torsional terms.

The second term in Eq. (1) represents pair-wise non-bonded interactions, i.e., the sum of van der Waals and Coulomb terms, $U_{ij}^{(nonb)}(r) = U_{ij}^{(LJ)}(r) + U_{ij}^{(Coul)}(r)$, and this is also used to model solvent–solute interactions

[1] Since the total number of monomers, $N = N_+ + N_-$, of these dendrimers approximately doubles with each generation, the composition, N_+/N is very close to half. Obviously also, reversing the charges here will produce an exactly identical system.

[2] Note that in this paper we use an extra factor of 3 as compared to Refs. [6,7] for a simpler comparison with the Edwards–de Gennes polymer model.

implicitly. We use the standard Lennard-Jones form of the potential,

$$U_{ij}^{(LJ)}(r) = \begin{cases} +\infty, & r < d, \\ U_{ij}^{(0)}\left(\left(\frac{d}{r}\right)^{12} - \left(\frac{d}{r}\right)^{6}\right), & r > d, \end{cases} \tag{2}$$

where r is the distance between monomers i and j and d corresponds to the monomer diameter. For the sake of convenience, we will choose $d = \ell$. Here $U_{ij}^{(0)}$ is the dimensionless strength of the 'effective' Lennard-Jones interaction acting between monomers i and j. Note that this model contains a 'hard sphere' form of the repulsions. The use of this model is computationally advantageous, since attempted MC steps which would cause an overlap of monomers can be automatically rejected, without evaluating the energy of the move. Note that, henceforth, we define all energies in units of k_BT and distances in units of d.

In amphiphilic copolymers, there are two types of monomers, hydrophobic (H) and polar (P). We model the behaviour of these two types in aqueous solution with the following method incorporating the effect of the solvent into the Lennard-Jones term [11,12]. We choose the strength of the attractions between two hydrophobic monomers equal to a sufficiently large value, namely, $U_{HH}^{(0)} = 6k_BT$, corresponding to water being a poor solvent for hydrophobic monomers. The strength of the attractions between two polar monomers is then taken as being zero, $U_{PP}^{(0)} = 0$, corresponding to water being a good (athermal) solvent for polar monomers, which thus only experience hard sphere repulsions. Finally, we take the strength of the attractions between a hydrophobic monomer and a polar monomer as being the arithmetic mean of the two previous values, i.e., $U_{HP}^{(0)} = 3k_BT$ (see Refs. [12,13] and references therein).

The Coulomb part of the potential is given in terms of the charges $q_i \equiv |e|\varsigma_i$, where $\varsigma_i = \{+1, -\delta\}$ and $\delta \equiv N_+/N_- \gtrsim 1$, is chosen so that the whole dendrimer is electrically neutral,

$$U_{ij}^{(Coul)}(r) = \varsigma_i\varsigma_j\frac{l_B}{r}, \quad l_B \equiv \frac{e^2}{4\pi\varepsilon_0\varepsilon k_BT}. \tag{3}$$

The overall strength of the Coulomb interactions is thus characterised by a single parameter, the Bjerrum length l_B. As the system is neutral overall we do not consider counter-ions in this paper.

4. Homo-dendrimers in solvents of variable quality

A considerable number of simulation studies using either Molecular Dynamics (MD), Stochastic Dynamics (SD), or Monte Carlo (MC), both on- and off-lattice, whether atomistically detailed or coarse-grained, have been performed [6,14–23]. On a number of issues concerning homo-dendrimer conformations a consensus is emerging. For instance, the backfolding of the terminal generations and their monomer delocalisation within the dendrimer in a good solvent is now widely accepted. However, the bond stretching pattern as a function of the span does appear to be strongly dependent on the model of the bonded conformations adopted: harmonic springs, FENE potential or rigid bonds. We can remark only that while the latter two choices are very popular for the coarse-grained description, none of the fully atomistic chemically accurate force fields use them. The density profile of the monomers as measured from the centre-of-mass (COM) also appear to be fairly model-dependent. High densities at the core are often observed, but large-G homo-dendrimers in a good solvent can also develop a plateau region, some local minima and higher-order oscillations in the more sophisticated of the models [19,21,24,25].

Our own previous study, based on a minimalistic model of hard spheres with harmonic springs [6], does find a deep minimum ('cavity'), but only in homo-dendrimers with G higher than a critical value and in a good solvent. Such a minimum is located close to the COM, but not directly at it. The existence of such a cavity and the 'dense-core' vs 'hollow-core' pictures are still highly debated in the literature at the moment (see e.g., Refs. [20,25,26]). Our findings show that this really depends on the dendrimer size, solvent quality, model parameters, and, in practice, on the chemical specificity of the dendrimers under study. Thus, there may or may not be a cavity. The latter is considered an important feature for accommodating guest molecules, but by no means a necessary pre-requisite as, e.g., electrostatic association [9], could also be used. We would also like to emphasise that, in a rather poor solvent, the density distribution is essentially uniform and the object is

space-filling [6]. Thus, the existence of a cavity is, clearly, a function of the solvent quality and pH as well—something which is often forgotten in the debate.

Perhaps the highest level of disagreement between different studies is about the scaling law for the mean-squared (MS) radius of gyration of the homo-dendrimer vs its architecture parameters (see e.g., discussions in Refs. [10,17,22,23]). One may, strictly speaking, doubt whether this is a valid question at all, given relatively small sizes of chemically realisable dendrimers and an asymptotic nature ($N \to \infty$) of such laws for e.g., linear polymers. Thus, at best, one should talk about just 'apparent' exponents, which will always be somewhat dependent on the procedure used in fitting the data. It is quite possible also, that the good- and theta-solvent scalings are not as universal as one is used for linear polymers. These can and, probably, do depend somewhat on the model and the dendrimer structure. For example, we saw that the exponents depend on the topology in star polymers [27] validated by the renorm-group calculations and the model-dependence of polyelectrolytes is also well known. Nevertheless, one is still tempted to try to find some sort of a reasonable scaling law.

Our own view, at least for the simplest model which we have studied, is that the following scaling law for the radius of gyration of dendrimers which involves the two exponents v_G (at fixed G) and v_D (at fixed D) is valid:

$$R_g \sim D^{v_G}(F-1)^{v_D(G+1)} \sim D^{v_G - v_D} N^{v_D}, \tag{4}$$

where $v_G = v$, with $v \approx \frac{3}{5}$, $\frac{1}{2}$ and $\frac{1}{3}$. Here v stands for the inverse fractal dimension of an open chain in the good, ideal and poor solvents, respectively. This is well supported by our data from both the MC simulations in continuous space and the improved Gaussian Self-Consistent (GSC) theory. While this law agrees with the conclusions of Refs. [17,28] for v_G, we have obtained a rather different dependence on the number of generations, which, by the way, is an exponential dependence and not a power law, a point deserving to be mentioned clearly. For the second exponent, we have concluded that $v_D \approx v - \frac{1}{4} \simeq 0.338$ for the good solvent, and $v_D \approx v = \frac{1}{3}$ for the poor solvent. This result is consistent with Ref. [18]. Thus, in a poor solvent, we simply have $R_g \sim N^{1/3}$. However, our estimate of v_D for the good solvent is more accurate enabling us to state that v_D is certainly above, although quite close, to the poor solvent value $\frac{1}{3}$.

We have also concluded that the coil-to-globule transition for dendrimers is continuous and that for the theta-solvent the scaling law for R_g differs from that of the ideal dendrimer, in which $R_g \sim (DG)^{1/2}$ (this is an exact result for large G), having instead the exponential (and not a power law) G-dependence of the form given by Eq. (4) with $\frac{1}{3} \leqslant v_D \leqslant 3/5 - \frac{1}{4}$.

We also would like to make two more points regarding the attempts to find a good scaling law for R_g in the good- and theta-solvents. First, one has to use two parameters as just N is insufficient. Using N itself with something else should be done with proper care as approximately the same N could be achieved with $G+1$ and D, as well as with G and $2D$. Thus, N is not really an independent variable of either D and G, and so should be treated via a constraint. It is much simpler to use just D and G, which are independent variables describing the dendrimer architecture, and then one could rewrite the final result in terms of N if one wishes to do so.

Second, the MS radius of gyration is by far the most difficult quantity to reproduce in MD and SD simulations as compared to e.g., the exact result in the model of an ideal dendrimer with purely harmonic springs, in which case the GSC theory reproduces the exact analytical answer [6]. We have verified this for our MC data and we would encourage others to do this comparison for MD and SD simulations as well. The difficulties in the former two techniques lie in the issue of cyclic trajectories (non-ergodicity) and consequent effective entropy under-estimation (which controls the swelling vs the bonded interactions) of the finite-time integrators and thermostat implementations. Only the best of thermostats, such as e.g., Nosé–Hoover chains, are known to give accurate enough results. In SD techniques a very good choice of high-order stochastic integrators and good random number generators also become essential if one is to reproduce R_g very accurately, while most of the other observables are not as sensitive to these technical details.

We shall present some curves for the homo-dendrimer in the next section as a reference point for comparison with the co-dendrimers.

5. Ampholytic co-dendrimers

We start by estimating physically reasonable order of magnitude for the Bjerrum length. By taking the monomer charge equal to that of electron $\pm e$, the dielectric permittivity of water $\varepsilon = 80.5$, $T = 300\,K$ and the

Table 1
Values of the global conformational observables: MS radius of gyration, mean energy, heat capacity and the axes of inertia for the homo-dendrimers with $D = 2$ spacers and $G = 3, \ldots, 6$ generations and varied values of the Bjerrum length l_B (in d units)

System	R_g^2	E	$\frac{C_V}{k_B}$	λ_1	λ_2	λ_3
$l_B = 0,\ G = 3$	19.8	252.9	131	0.51	0.31	0.18
$G = 4$	32.0	524.3	275	0.48	0.32	0.20
$G = 5$	50.4	1069	562	0.45	0.33	0.22
$G = 6$	79.3	2163	1229	0.43	0.33	0.24
$l_B = 0.5,\ G = 3$	19.2	253.8	138	0.52	0.32	0.16
$G = 4$	30.9	527.1	289	0.48	0.33	0.19
$G = 5$	48.4	1074	595	0.45	0.33	0.22
$G = 6$	75.4	2171	–	0.43	0.33	0.24
$l_B = 1,\ G = 3$	17.8	240.0	147	0.53	0.32	0.15
$G = 4$	28.7	499.4	313	0.49	0.32	0.19
$G = 5$	44.8	1018	637	0.46	0.33	0.21
$G = 6$	69.9	2056	–	0.43	0.33	0.24
$l_B = 3,\ G = 3$	14.5	141.0	180	0.54	0.31	0.15
$G = 4$	23.2	307.8	377	0.50	0.32	0.18
$G = 5$	35.7	637.3	758	0.47	0.32	0.21
$G = 6$	54.8	1292	1559	0.44	0.33	0.23

monomer diameter as 1 nm we shall arrive at the value of $l_B \simeq 0.69\,d$. Thus, we shall study the following values of $l_B = 0.5, 1, 3$ to model different reasonable charge values and distinct polar solvents, as well as compare these results to the neutral homo-dendrimer case ($l_B = 0$). Here we shall restrict ourselves to the purely repulsive case $U^{(0)} = 0$.

To understand the effect of increasing the Bjerrum length the following observables characterising the conformations of these dendrimers are reported in Table 1: the MS radius of gyration R_g^2, the mean energy E, the heat capacity $C_V/k_B \equiv (\Delta E)^2/(k_B T)^2$, and the axes of inertia, which are defined in Ref. [6]. Also we plot the RMS (root mean-squared) distances of monomers from the COM[3] in Fig. 1, the RMS distances between the consecutive monomers along the span in Fig. 2, as well as the partial densities of both types of charges and the total densities in Figs. 3–5.

The MS radius of gyration at a fixed G monotonically decreases on increasing l_B as evident from Table 1. This is related to the increased attraction between the distinctly charged monomers. Interestingly, the mean energy at a fixed G first starts to weakly increase with l_B, which is due to the increase in the bond stretching (this is quite clear also from Fig. 2), but then starts to dramatically decrease with further increases in l_B due to the dominant attractive electrostatic negative contribution. The heat capacity appears to slowly increase with l_B at a fixed G due to increased competition between the spring and electrostatic contributions. Increasing the number of generations G at a fixed l_B always leads to more spherical shapes, as in the case of the homo-dendrimer. At a fixed G, increasing l_B does not seem to seriously affect λ_2, but leads to some increase of λ_1 with an attendant decrease in λ_3, the shape of the ampholytic co-dendrimer therefore monotonically becoming more elongated. This effect is much more pronounced in small G co-dendrimers due to larger shape fluctuations in the more compact objects.

From Fig. 1 it is apparent that increasing l_B decreases the RMS distances from the COM for the peripheral (positively charged) monomers, as well as for some of their nearest neighbours, which are negatively charged. This is due to the increased attraction of the positive units towards the negatively charged monomers. Speaking of the negatively charged monomers, increasing the Bjerrum length at first leads to an increase in $R^{(cm)}$ due to the likewise charge repulsions. This trend, however, is later reversed when the screening of the

[3]Note that here we define all distances like this without the 'historical' factor of $\frac{1}{3}$ as compared to Refs. [6,7], i.e., $R_{ij} \equiv \sqrt{\langle(\mathbf{X}_i - \mathbf{X}_j)^2\rangle}$.

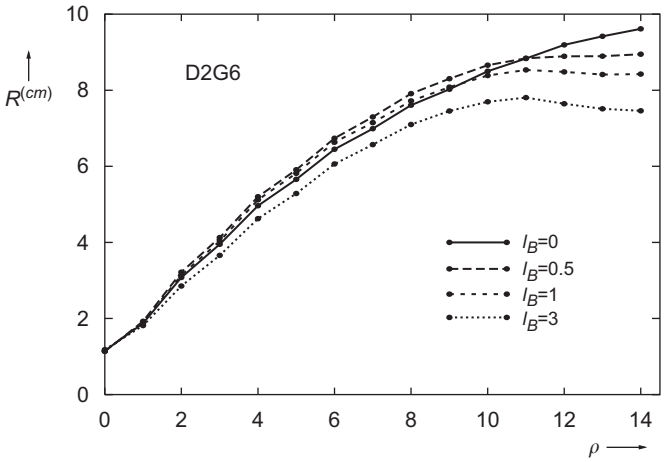

Fig. 1. Plot of the RMS distances of monomers from the centre-of-mass vs the span index ρ for *D2G6* dendrimer with varied Bjerrum length values (in d units here and below).

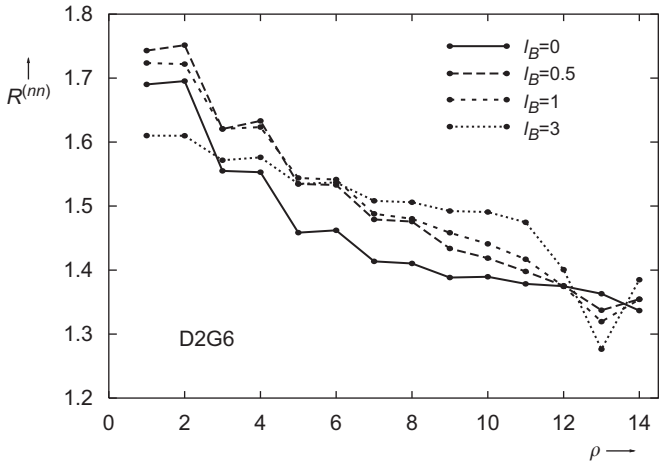

Fig. 2. Plot of the RMS distances between the consecutive monomers vs the span index for *D2G6* dendrimer with varied Bjerrum length values (in d units here and below).

negatively charged core by the backfolding positively charged ends of the co-dendrimer starts to dominate. The latter effect is especially pronounced for the largest considered value of $l_B = 3\,d$ (dotted line in Fig. 1).

It is also instructive to analyse the bond stretching between consecutively connected monomers on increasing l_B (see Fig. 2). The homo-dendrimer case ($l_B = 0$) was discussed in detail in Ref. [6] and is presented for reference in this figure by the solid line. Its main features are: the strongest stretching of the bonds adjacent to the core (due to 'entropic pull') and a step-like descent with the bonds connecting monomers within the same generations being nearly equal. At the same time, the outermost bonds being stretched the least. Increasing l_B to relatively small values (long-dashed line) leads to a straightforward result: an increase in the bond stretching connecting equally charged monomers and a decrease in the bond stretching between the oppositely charged monomers (at $\rho = 13$ in the figure). Further increases in l_B reverse this trend near the core (for values of ρ up to 5), while continuing to increase the bond stretching for the other (likewise charged) monomers and leading to an even stronger decrease in the bond stretching at the charge interface.

In order to interpret these observations better let us consider the partial and total monomer densities in Figs. 3–5. Fig. 3 is presented here for reference purposes, while similar quantities for the homo-dendrimer have

been discussed in Ref. [6]. In the present model with harmonic bonds and hard spheres, small G dendrimers (the inset) have densities monotonically decreasing with the increasing distances from the COM, whereas large G dendrimers (the main body) possess a non-monotonic density dependence with a local minimum ('cavity') not far from the COM. In Ref. [6] we interpreted this in terms of the backfolding of the terminal monomers and we believe this observation may reconcile the arguments between the proponents of the 'dense-core' vs the 'hollow-core' pictures [26,20].

An increase of l_B to the value of 1 d (Fig. 4), interestingly, produces an overcharged positive charge area near the location of the minimum in $g^{(1)}_{(tot)}$ for large G dendrimers, which is followed by overcharged negative charge area and concluded by the positively charged periphery. This phenomenon bears a striking resemblance to the overcharged layers in the charged colloid particles with counter-ion systems [29], for which many double- and multi-layer theories have been developed, starting from the classical DLVO theory. Notice that for small G dendrimers (the inset) this effect does not as yet occur, nor is there a local minimum ('cavity') in the density profile as in the case of the homo-dendrimer. Finally, from Fig. 5 it is evident that the partial

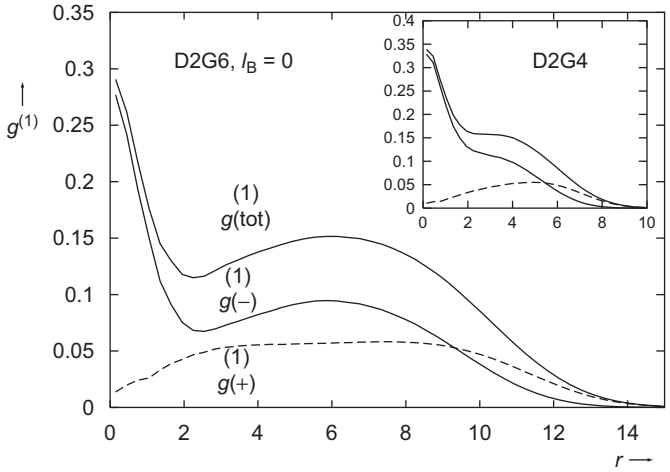

Fig. 3. Plots of the total $g^{(1)}_{(tot)}$ and partial $g^{(1)}_{(\pm)}$ densities of monomers in $D2G6$ and $D2G4$ (inset) dendrimers vs the radial separation from the centre-of-mass for the value $l_B = 0$.

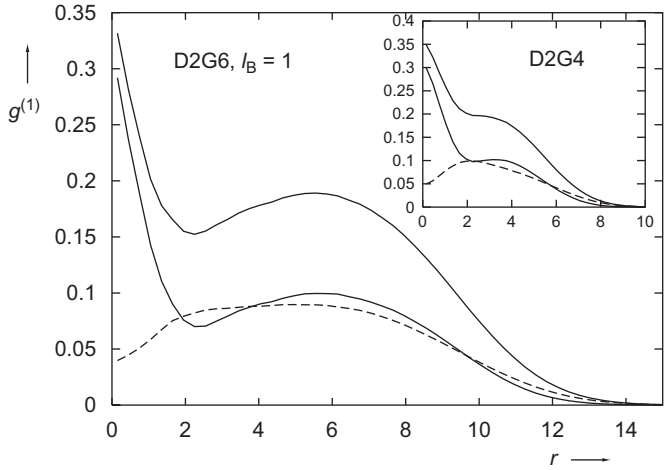

Fig. 4. Plots of the total $g^{(1)}_{(tot)}$ and partial $g^{(1)}_{(\pm)}$ densities of monomers in $D2G6$ and $D2G4$ (inset) dendrimers vs the radial separation from the centre-of-mass for the value $l_B = 1$.

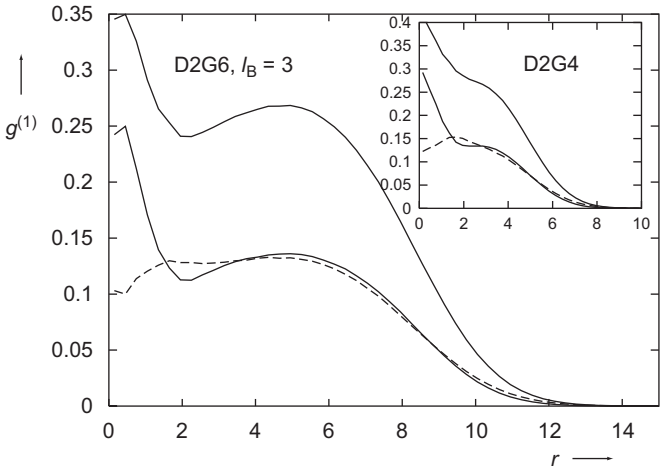

Fig. 5. Plots of the total $g^{(1)}_{(tot)}$ and partial $g^{(1)}_{(\pm)}$ densities of monomers in *D2G6* and *D2G4* (inset) dendrimers vs the radial separation from the centre-of-mass for the value $l_B = 3$.

densities of both monomer types converge more and more towards each other in the range of large separations, leading to a better screening of charges. Therefore, for such large *G* dendrimers only two layers of charges are well discernible (i.e., the negatively charged core, followed by a positively charged layer and concluded by a nearly screened area of weakly fluctuating charge). From this discussion it is also clear that the backfolding of the positive charges from the periphery effectively reduces the repulsions, and thus the inner bond stretchings (dotted line in Fig. 2), within the negatively charged core.

6. Conclusions

In this paper we have reviewed the conformational properties of homo-dendrimers in solvents of variable quality and we have also studied ampholytic co-dendrimers. For the former, which are used for comparison with the latter more complex co-dendrimers, we have discussed various features, which are either in consensus or being widely debated in the literature. We have also tried to understand the possible reasons for the disagreements, which seem to mostly relate to their model-dependence for these highly congested and sensitive dendrimer systems.

For ampholytic co-dendrimers, we have observed here a number of interesting novel effects for the RMS monomer distances from the centre-of-mass, RMS bond lengths, as well as for the partial and total monomer densities, stemming from the likewise charge repulsion and from the screening and overcharging phenomena due to the backfolding of the oppositely charged terminal monomers. We have also observed the electrostatic elongation of the average shapes of these co-dendrimers expressed in terms of their axes of inertia.

We hope that our results would allow one to reconcile some of the disparate predictions from previous simulation studies causing the current controversy in the literature. The unusual features of the dendrimers described here make them even more appealing for future applications ranging from catalysis, supramolecular chemistry, rheology modifiers, to drug delivery and other areas of biotechnology.

Acknowledgments

We are grateful to Professor Fabio Ganazzoli, Gillian Flanagan, Marese O'Brien, Tina O'Farrell and Dr Ronan Connolly for interesting discussions. Support from the IRCSET basic research Grant SC/02/226 is also acknowledged.

References

[1] O.A. Matthews, A.N. Shipway, J.F. Stoddart, Prog. Polym. Sci. 23 (1998) 1;
S.M. Grayson, J.M.J. Fréchet, Chem. Rev. 101 (2001) 3819;
A.W. Bosman, H.M. Janssen, E.W. Meijer, Chem. Rev. 99 (1999) 1665;
G.R. Newkome, C.N. Moorefield, F. Vögtle, Dendritic Molecules: Concepts, Synthesis, Perspectives, Verlag-Chemie, Weinheim, 1996;
D.A. Tomalia, A.M. Naylor, W.A. Goddard III, Angew. Chem. Int. Ed. Engl. 29 (1990) 138.

[2] M. Liu, J.M.J. Fréchet, Pharm. Sci. Technol. Today 2 (1999) 393;
L.J. Twyman, A.E. Beezer, R. Esfand, M.J. Hardy, J.C. Mitchell, Tetrahedron Lett. 40 (1999) 1743;
M. Liu, K. Kono, J.M.J. Fréchet, J. Controlled Release 65 (2000) 121;
C.J. Hawker, K.L. Wooley, J.M.J. Fréchet, J. Chem. Soc. Perkin Trans. 1 (1993) 1287.

[3] G.E. Oosterom, J.N.H. Reek, P.C.J. Kamer, P.W.N.M. van Leuwen, Angew. Chem. Int. Ed. 40 (2001) 1829.

[4] F. Zeng, S.C. Zimmerman, Chem. Rev. 97 (1997) 1681.

[5] J.S. Moore, Acc. Chem. Res. 30 (1997) 402.

[6] E.G. Timoshenko, Yu.A. Kuznetsov, R. Connolly, J. Chem. Phys. 117 (2002) 9050.

[7] R. Connolly, E.G. Timoshenko, Yu.A. Kuznetsov, Macromolecules 37 (2004) 7381.

[8] M.E. Piotti, F. Rivera Jr., R. Bond, C.J. Hawker, J.M.J. Fréchet, J. Am. Chem. Soc. 121 (1999) 9471;
A.I. Cooper, J.D. Londono, G. Wignall, J.B. McClain, E.T. Samulski, J.S. Lin, A. Dobrynin, M. Rubinstein, A.L.C. Burke, J.M.J. Fréchet, J.M. DeSimone, Nature 389 (1997) 368;
S. Stevelmans, J.C.M. van Hest, J.F.G.A. Jansen, D.A.F.J. van Boxtel, E.M.M. de Brabander-van den Berg, E.W. Meijer, J. Am. Chem. Soc. 118 (1996) 7398;
A.P.H.J. Schenning, C. Elissen-Román, J.-W. Weener, M.W.P.L. Baars, S.J. vander Gaast, E.W. Meijer, J. Am. Chem. Soc. 120 (1998) 8199;
Y. Sayed-Sweet, D.M. Hedstrand, R. Spindler, D.A. Tomalia, J. Mater. Chem. 7 (1997) 1199;
Y. Pan, W.T. Ford, Macromolecules 32 (1999) 5468.

[9] P. Welch, M. Muthukumar, Macromolecules 31 (1998) 5892;
P. Welch, M. Muthukumar, Macromolecules 33 (2000) 6159.

[10] F. Ganazzoli, R. La Ferla, G. Terragni, Macromolecules 33 (2000) 6611;
F. Ganazzoli, R. La Ferla, G. Raffaini, Macromolecules 34 (2001) 4222.

[11] R. Connolly, E.G. Timoshenko, Yu.A. Kuznetsov, J. Chem. Phys. 119 (2003) 8736.

[12] F. Ganazzoli, Yu.A. Kuznetsov, E.G. Timoshenko, Macromol. Theory Simulations 10 (2001) 325.

[13] E.G. Timoshenko, Yu.A. Kuznetsov, J. Chem. Phys. 112 (2000) 8163.

[14] A.N. Naylor, W.A. Goddard III, G.E. Kiefer, D.A. Tomalia, J. Am. Chem. Soc. 111 (1989) 2339.

[15] R.L. Lescanec, M. Muthukumar, Macromolecules 23 (1990) 2280.

[16] M.L. Mansfield, L.I. Klushin, Macromolecules 26 (1993) 4262.

[17] Zh.Yu. Chen, Sh.-M. Cui, Macromolecules 29 (1996) 7943.

[18] M. Murat, G.S. Grest, Macromolecules 29 (1996) 1278.

[19] P.K. Maiti, T. Cagin, G. Wang, W.A. Goddard III, Macromolecules 37 (2004) 6236.

[20] H.M. Harreis, C.N. Likos, M. Ballauff, J. Chem. Phys. 118 (2003) 1979.

[21] S. Rathgeber, T. Pakula, V. Urban, J. Chem. Phys. 121 (2004) 2840.

[22] G. Guipponi, D.M.A. Buzza, J. Chem. Phys. 120 (2004) 10290.

[23] Y.J. Sheng, S.Y. Jiang, H.K. Tsao, Macromolecules 35 (2002) 7865.

[24] T. Terao, T. Nakayama, Macromolecules 37 (2004) 4686.

[25] I.O. Götze, C.N. Likos, Macromolecules 36 (2003) 8189.

[26] T.C. Zook, G.T. Pickett, Phys. Rev. Lett. 90 (2003) 015502.

[27] E.G. Timoshenko, Yu.A. Kuznetsov, R. Connolly, J. Chem. Phys. 116 (2002) 3905.

[28] P. Biswas, B.J. Cherayil, J. Chem. Phys. 100 (1994) 3201.

[29] J. Israelachvili, Intermolecular and Surface Forces, Academic Press, London, 1991.